Available online at www.eccomasproceedia.org
Eccomas Proceedia COMPDYN (2023) 854-861

ECCOMAS Proceedia

COMPDYN 2023
9th ECCOMAS Thematic Conference on
Computational Methods in Structural Dynamics and Earthquake Engineering
M. Papadrakakis, M. Fragiadakis (eds.)
Athens, Greece, 12-14 June 2023

EXPERIMENTAL PULL-OUT BEHAVIOR OF HELICOIDAL STEEL BARS IN MASONRY

Manuela Scamardo[1], **Sara Cattaneo**[1] **and Pietro Crespi**[1]

[1] Department of Architecture, Built Environment and Construction Engineering, Politecnico di Milano
20133 Milan, Italy
{manuela.scamardo, sara.cattaneo, pietro.crespi}@polimi.it

Abstract

When dealing with the retrofitting of historical heritage buildings, the improvement of the structural behavior should be weighed against the compatibility of the designed interventions, in order to preserve the architectural value, avoiding irreversible damages. Helicoidal stainless steel bars are becoming widely used for the retrofitting of historical masonry buildings for crack stitching or to improve the transversal connection between different structural elements, even if very few studies on their mechanical behavior are presented in the scientific literature. In this paper, an experimental study on the pull-out behavior of helicoidal stainless steel bars installed into the masonry is presented. The investigated parameters were the masonry wall strength (by considering two different bricks and two different mortar strengths), the embedment depth (100, 200 and 400 mm), the position of the bar (brick, T-joint, face or side of the wall) and the orientation of the bar (0° or 45°). The bar performances were assessed under monotonic tension and cyclic axial loading. The bar diameter adopted for all the tests was 12 mm. Results showed very good performance with reliable results associated to low coefficient of variation of the loads and with a very limited damage of the base material. The load-displacement curves showed a good ductility, an excellent superposition between monotonic and cyclic tests, with an extended plateau. Among the different investigated parameters, the position within the wall was the most influential one, with higher loads associated to the location of the bar in middle of the brick.

Keywords: Repair and strengthening, helicoidal steel bars, masonry heritage buildings, pull-out tests.

ISSN:2623-3347
Peer-review under responsibility of the organizing committee of COMPDYN 2023.
doi: 10.7712/120123.10440.20822

1 INTRODUCTION

The greatest part of the Italian built heritage is made of masonry buildings. Despite their good performance with respect to vertical loads, masonry structures have demonstrated to be vulnerable to the horizontal loads. Indeed, extensive damages have been recorded on churches, towers and palaces during the Italian recent seismic events [1-3], with significant losses of architectural, historical and cultural value.

Many efforts have been dedicated by the scientific community to study and develop innovative retrofitting techniques, particularly tailored to the specific needs of heritage structures, to improve their seismic performance [4-6]. According to the Italian Guidelines for the preservation of cultural heritage [7], the structural interventions should comply with some recognized conservation principles which includes minimal (non-invasive) interventions, material compatibility and reversibility of repair.

One crucial feature which helps the seismic response of masonry structures is the good connection between the bearing orthogonal walls, that, together with the presence of rigid floor diaphragms, can significantly improve the box-behavior, achieving a more favorable distribution of horizontal loads. When the quality of the wall-to-wall intersections is not acceptable (due to bad workmanship or as a consequence of earthquake damage), the structural connection can be improved by introducing proper connecting systems. Nowadays, metallic anchors inserted into a predrilled hole injected with grout or adhesive are commonly applied [8-9]. Nevertheless, in case of heritage buildings, this strengthening system conflicts with the conservation principles mentioned above (it is not reversible and compatibility problems may arise depending on the chosen injecting material).

More recently, helicoidal stainless steel bars have become very popular for both crack stitching and to improve the connections between structural elements. The main reason of this popularity is due to the fact that the installation of the bars is made without any need of binder (resin or grout), which becomes a great advantage in terms of sustainability and compatibility when dealing with heritage masonry buildings. Even though these bars are made available in the market by several manufacturers, very few studies on their mechanical behavior are presented in the scientific literature [10-11].

This paper presents the results of an experimental study on the pull-out behavior of helicoidal stainless steel bars installed into the masonry. A bar diameter of 12 mm was considered. The bar performances were assessed under monotonic tension and cyclic axial loading. Several design parameters were investigated such as the masonry wall strength, the embedment depth, the position of the bar and the orientation of the bar.

2 EXPERIMENTAL PROGRAM

2.1 Materials

The mechanical properties of the stainless steel helicoidal bar declared by the manufacturer [12] are reported in Table 1.

Nominal drill bit diameter (mm)	Outer diameter (mm)	Nominal section (mm^2)	Tensile rupture load (kN)	Yielding load (kN)	Elastic modulus (MPa)
8	12	15.1	18.9	16.1	>122

Table 1: Geometrical and mechanical properties of helicoidal bar "Heli-Brick"

The bars were installed into 8 mm diameter pre-drilled holes, after cleaning them by blowing compressed air along the embedment depth. As base material, two different masonry typologies were considered: a weak (W) wall, made by solid bricks with mean compressive strength of 25 MPa and M2.5 mortar, with dimension of 1290×1290×250 mm and joint thickness of 10 mm; a strong (S) wall, made by solid bricks with mean compressive strength of 34 MPa and M5 mortar, with dimensions of 1000×1000×600 mm and joint thickness of 20 mm.

2.2 Experimental set up

A special system was constructed to clamp the helicoidal bar (Fig.1a), completed by an horizontal bar to prevent the rotation during the test (Fig.1b) (phenomenon also observed by other authors [11]). Unconfined displacement controlled tensile tests were performed with a test rig equipped with a 25 kN load cell. Two LVDTs (gage length 100 mm) were placed symmetrically to the anchor axis to measure the displacements.

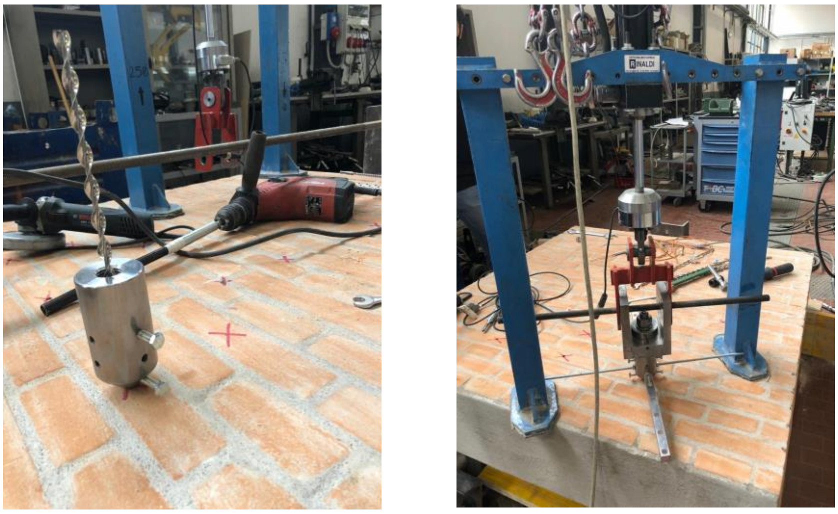

(a) (b)

Figure 1: (a) bar with clamping device and (b) test rig with anti-rotation system.

2.3 Test plan and load protocol

The aim of the experimental study was to evaluate the performance of the bar under tension considering the influence of the following parameters:

- wall strength (weak “W” or strong “S”);
- embedment length (100, 200, and 400 mm);
- different position of the bar (in the middle of the brick “M” or in the T-joint “TJ”, on the face “F” of the wall or on the side “S”);
- orientation of the bar (0° or 45° in the horizontal “H” or vertical “V” plane).

The bar performances were assessed first under monotonic tension. On the basis of monotonic tests results, a protocol for cyclic tests was defined. In particular, reasonable target displacement levels were defined (0.25, 0.5, 1.0, 2.0, 3.5, 5, 7, 9, 11, 14, 17, 20, 25, 30, 40, 50, 60 mm) and 3 cycles for each displacement level were performed. Two different unloading conditions were considered: down to zero tension load (“C”) and down to zero displacement under compression load (“CC”).

A total of 48 tests were performed, three for each configuration except for the case where the coefficient of variation of the load was higher than 15%, in which case the number of tests was increased up to 5.

3 EXPERIMENTAL RESULTS

Table 2 shows the results of the tests, grouped for the different configurations, in terms of average ultimate load N_m with the corresponding coefficient of variation $v(N_m)$, and the value of displacement at the peak load δ_p with the respective coefficient of variation $v(\delta_p)$. Considering the previously introduced abbreviation, the test denomination is defined according to the following code: HE12 - type of wall (S or W) – position (F or S) - position within the wall (M or TJ) – orientation angle (0°, 45°H or 45°V) – embedment length (100, 200 or 400) – type of test (C or CC, added only for cyclic tests).

Connector pull-out was the failure mode observed in all the cases, except in some cyclic tests without residual displacements, where the compression caused the bar buckling and a consequent steel failure (Fig. 2a). After each test, the damage on the masonry was very limited (Fig. 2b).

Test denomination	# tests	N_m kN	$V(N_m)$ %	δ_p mm	$v(\delta_p)$ %	$\delta_{0.5Nm}$ mm	$v(\delta_{0.5Nm})$ %
HE12-W-F-M-0-100	3	5.54	3.2	15.46	8.7	1.79	1.6
HE12-W-F-M-0-200	3	6.84	5.1	18.60	32.4	4.27	23.7
HE12-W-F-M-0-200-CC	4	6.84	1.7	16.90	17.1	-	-
HE12-W-F-M-0-200-C	3	5.23	6.8	15.65	15.65	-	-
HE12-W-S-M-0-200	3	7.03	3.6	20.97	27.0	3.67	26.1
HE12-W-F-TJ-0-200	5	5.25	4.4	20.29	14	4.12	30.9
HE12-W-F-TJ-0-200-CC	3	3.87	11.1	9.66	15.04	-	-
HE12-W-F-TJ-0-200-C	3	6.44	2.0	17.23	17.23	-	-
HE12-W-F-TJ-45H-200	5	5.32	16.2	17.40	9.0	2.63	93.0
HE12-W-F-TJ-45V-200	3	5.71	9.1	22.71	37.7	1.56	36.0
HE12-S-F-M-0-400	3	8.20	3.5	17.08	12.8	4.79	55.9
HE12-S-F-TJ-0-400	3	7.19	8.4	36.78	21.8	4.14	58.2
HE12-W-S-TJ-0-400	3	6.59	4.9	30.16	55.3	4.16	124.1
HE12-W-S-TJ-45V-400	4	7.60	4.2	36.49	25.4	4.54	72.4

Table 2: Test results

(a) (b)

Figure 2: (a) steel failure due to buckling and (b) limited damage on masonry.

4 DISCUSSION

In general, it can be noted from Table 2 that all tests showed a low coefficient of variation of the ultimate load, while the displacement values exhibited a higher scatter.

Considering the monotonic test results, the bar installed into the brick showed higher strengths with lower coefficients of variation compared to bars installed in the T-joint position. Moreover, as evident in the load-displacement curves reported in Figure 3a-b, the installation in the brick also guaranteed a more ductile behavior, with a plateau whose length increases with the embedment depth (Fig. 3a-c). A higher embedment length means also a higher maximum load. No specific differences were observed in tests performed on the side and on the face of the wall (Fig. 3a-d).

The strength of the wall seems to have a beneficial effect on the ultimate load as proved by test HE12-W-S-TJ-0-400 vs. HE12-S-F-TJ-0-400, in which the mean peak load increases from 6.6 kN to 7.2 kN from the weak to the strong wall (see Table 2). When the (vertically) inclined configuration is considered (HE-12-W-S-TJ-400-45V), the mean resistance further increases to 7.6 kN. This is probably due to the fact that the percentage of bricks that the bar intersects is higher than in the other configurations. A clear influence on the maximum load was not detected for the inclination of the bar in the horizontal plane.

Considering the configuration HE12-W-F-M-0-200, Figure 4 shows the displacement vs. time and the load vs. displacement for the cyclic tests to zero tension load (Fig. 4a-b) and to zero displacement (Fig. 4c-d). Figure 5 represents instead the peak load associated to each cycle as a function of the displacement, in the two different loading protocols.

In the cyclic tests to zero tension load, a high residual displacement remained after the first cycle of each displacement level (while after second and third cycles, the residual displacement was similar to the one of the first cycle). A higher peak load was also recorded in the first cycle, with a degradation of the resistance in the following ones.

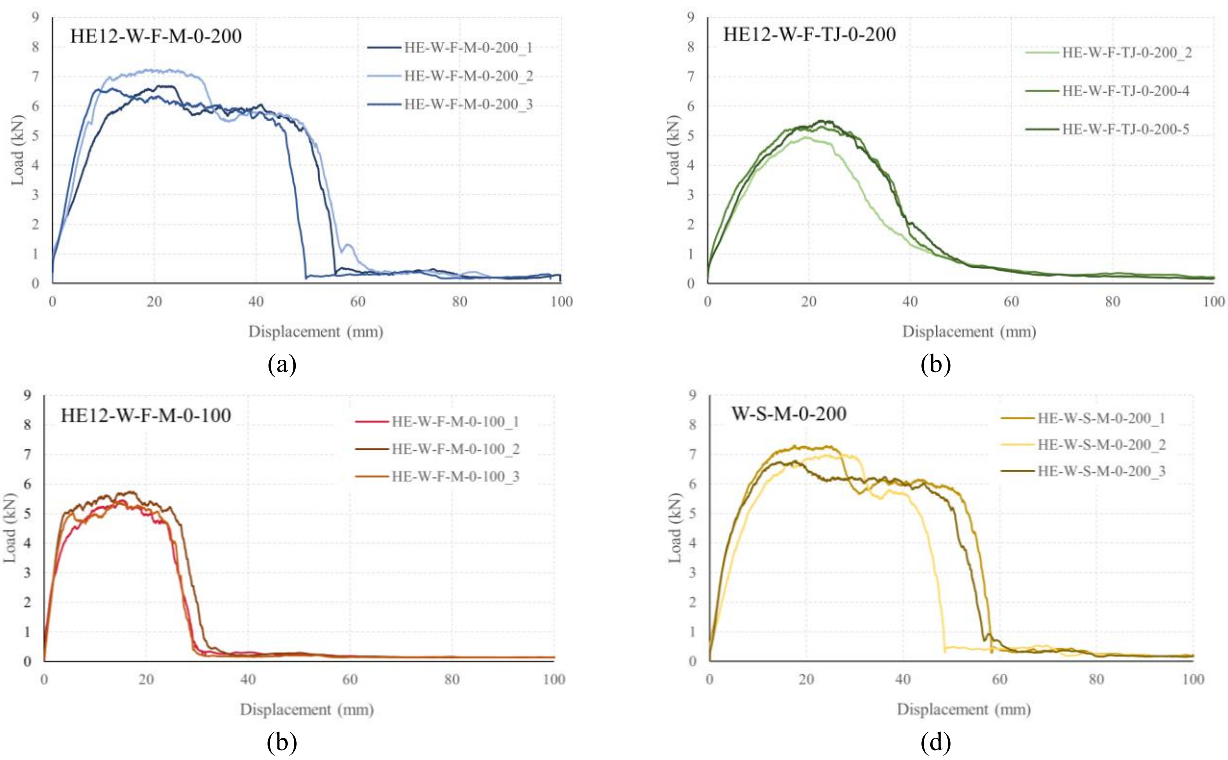

Figure 3: Load vs. displacement curve (a) in the brick, (b) in the T-joint, (c) for lower embedment depth and (d) on the side of the wall.

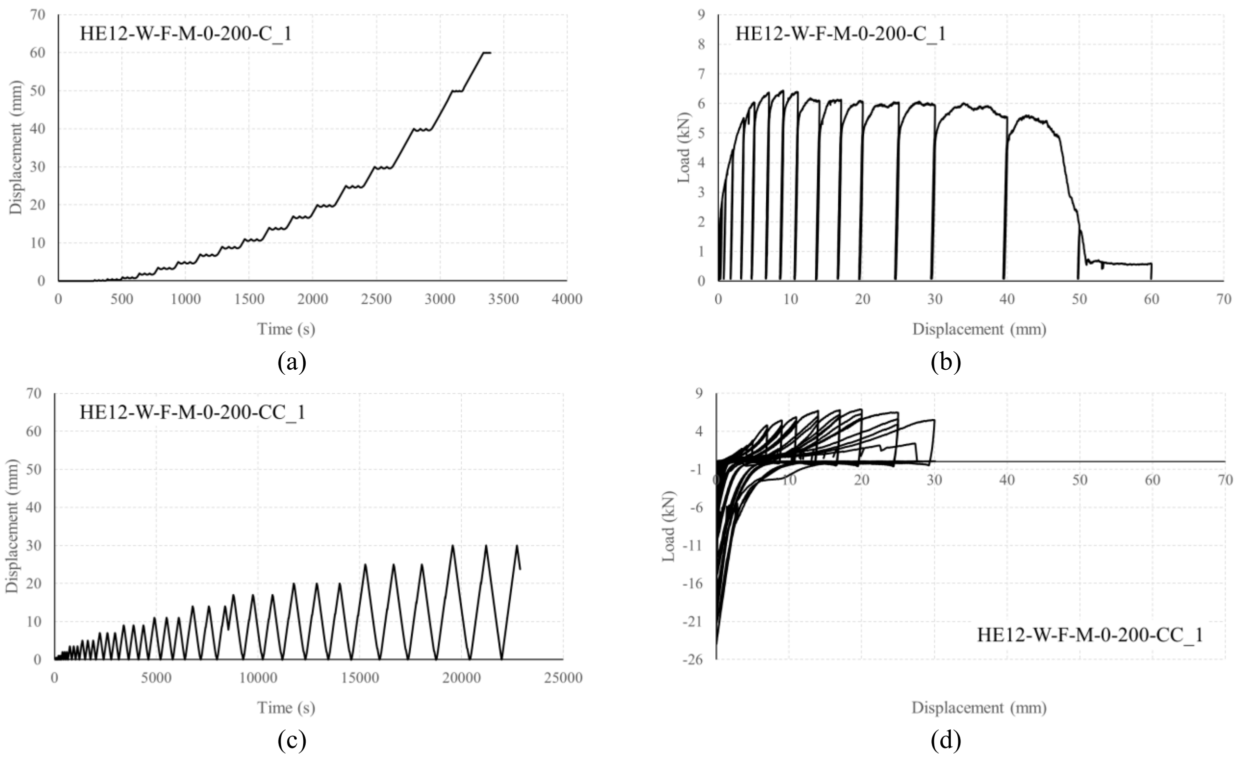

Figure 4: Displacement vs. time and load vs. displacement curve for the cyclic test to zero tension load (a-b) and to zero displacement (c-d).

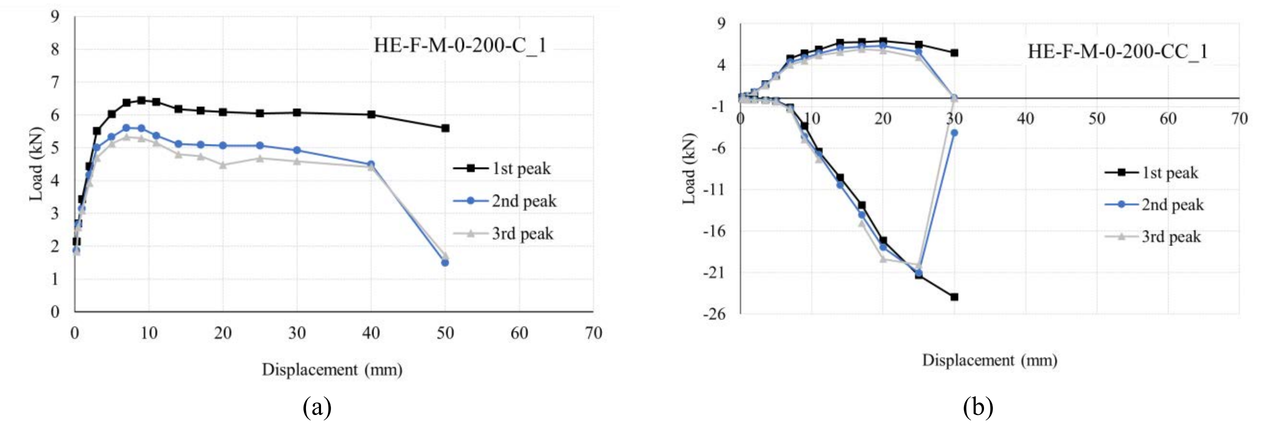

Figure 5: Peak load for each cycle for cyclic tests (a) to zero load and (b) to zero displacement.

In the cyclic tests to zero displacement, before the application of the compression load, similar results were found, both in terms of load and displacement, with respect to the tests with residual displacement. When the bar underwent to compression, buckling phenomena were observed and, with the increasing of the number of cycles, the axis of the bar misaligned and the bar was pushed sidewards (Fig. 2a). At the end of the test, a steel failure of the bar was observed under tension load. The load degradation after the first cycle was more limited with respect to the one recorded in the cyclic tests with residual displacement.

Figure 6 shows a comparison between the results obtained from the monotonic and cyclic tests, in the brick and in the T-joint. For the bar installed in the middle of the brick (Fig. 6a), the maximum load is not influenced by the test protocol, while considering the T-joint position (Fig. 6b), the maximum load in the cyclic test to zero displacement resulted lower than the one obtained in the other protocols. In general, the maximum displacement reached in the cyclic tests to zero displacement resulted lower with respect to the other protocols. Nevertheless, it was large enough to guarantee a good structural behavior.

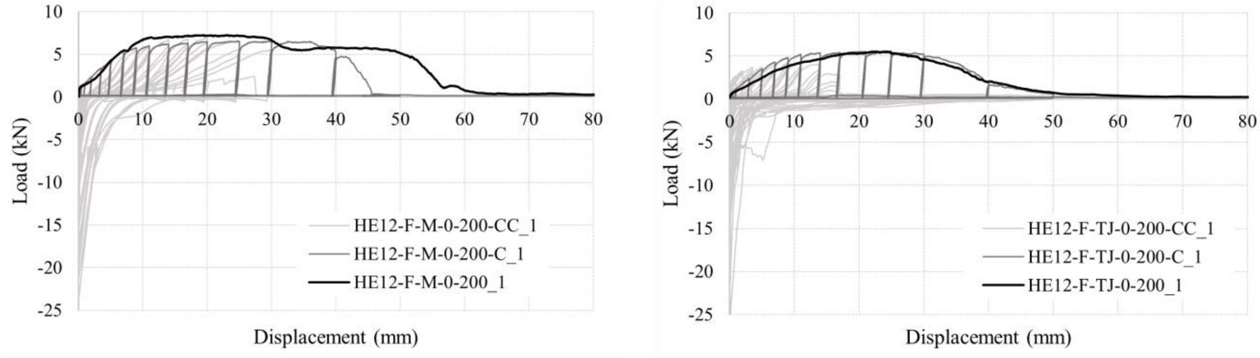

Figure 6: Comparison between the monotonic, cyclic to zero tension load and cyclic to zero displacement tests for bar (a) in the brick and (b) in the T-joint.

5 CONCLUSIONS

The paper presented the results of an experimental program to characterize the structural behavior of stainless steel helicoidal bars, very popular for the retrofitting of historical masonry buildings. Pull-out tests under monotonic and cyclic protocols were performed, investigating the influence of several parameters (such us the position of the bar, the embedment depth or the wall strength) on the bar behavior. The results showed very good performance with reliable results associated to low coefficient of variation of the loads and with a very limited damage of the base material. The load-displacement curves showed a good ductility, especially for the installation of the bar in the brick, and an excellent superposition between monotonic and cyclic tests. Among the different investigated parameters, the position within the wall face was the most influential one, with higher loads associated to the location of the bar in the middle of the brick.

REFERENCES

[1] S. Lagomarsino, Damage assessment of churches after L'Aquila earthquake (2009), *Bulletin of Earthquake Engineering*, **10**, 73–92, 2012.

[2] M. Valente, G. Barbieri, L. Biolzi, Damage assessment of three medieval churches after the 2012 Emilia earthquake, *Bulletin of Earthquake Engineering*, **15**, 2939–2980, 2017.

[3] F. Ubertini, N. Cavalagli, A. Kita, G. Comanducci, Assessment of a monumental masonry bell-tower after 2016 Central Italy seismic sequence by long-term SHM, *Bulletin of Earthquake Engineering*, **16**, 775–801, 2018.

[4] F. Yavartanoo, T.H.K. Kang, Retrofitting of unreinforced masonry structures and considerations for heritage-sensitive constructions, *Journal of Building Engineering,* **49**, 103933, 2022.

[5] S. De Santis, G. de Felice, F. Roscini, Retrofitting of Masonry Vaults by Basalt Textile-Reinforced Mortar Overlays, *International Journal of Architectural Heritage*, **13**, 1061-1077, 2019.

[6] N. Longarini, P. Crespi, M. Scamardo, Numerical approaches for cross-laminated timber roof structure optimization in seismic retrofitting of a historical masonry church, *Bulletin of Earthquake Engineering*, **18**, 487-512, 2020.

[7] Consiglio Superiore dei Lavori Pubblici, Direttiva inerente l'"Allineamento delle Linee Guida per la valutazione e la riduzione del rischio sismico del patrimonio culturale alle nuove Norme Tecniche sulle costruzioni", 2010.

[8] S. Paganoni, D. D'Ayala, Testing and design procedure for corner connections of masonry heritage buildings strengthened by metallic grouted anchors, *Engineering Structures*, **70**, 278–293, 2014.

[9] M. Corradi, A. Borri, E. Poverello, G. Castori, The use of transverse connectors as reinforcement of multi-leaf walls, Materials and Structures, **50**, 114, 2017.

[10] M. Candela, A. Borri, M. Corradi, L. Righetti, Effect of transversal steel connectors on the behavior of rubble stone-masonry walls: Two case studies in Italy, in: *Brick and Block Masonry: Trends, Innovations and Challenges - Proceedings of the 16th International Brick and Block Masonry Conference (IBMAC 2016)*, 2016.

[11] C. Gentilini, F. Finelli, V.A. Girelli, E. Franzoni, Pull-out behavior of twisted steel connectors employed in masonry: The influence of the substrate, *Construction and Building Materials*, **274,** 122115, 2021.

[12] C. Gentilini, F. Finelli, C. Carloni, An experimental study of the bond behavior of twisted steel bars embedded in mortar cylinders and in the joints of masonry wallettes, *Construction and Building Materials*, **316**, 125795, 2022.

[13] Hilti Heli-Brick documentation and instructions for use, Hilti Italia S.p.A.